OPEN ACCESS

International
Journal
Of Modern Engineering Research (IJMER)

Effects of Continuous Cooling On Impact and Micro Structural Properties of Low Carbon Steel Welded Plate

Aweda, E. O.[1], Dauda, M.[2], Dagwa, I. M[3]. , Dauda, E.T[4].
[1,2]*Department of Mechanical Engineering Faculty of Engineering Ahmadu Bello University Zaria.*
[3]*Department of Mechanical Engineering Faculty of Engineering University of Abuja Abuja*
[4]*Department of Materials and Metallurgy Engineering Faculty of Engineering Ahmadu Bello University Zaria.*

ABSTRACT: *Some mechanical properties and microstructural analysis were conducted on shielded metal arc weldments of low carbon steels in some simulated environments. Specimens were prepared and subjected to welding and continuous cooling at the same time at various positions. Results obtained for impact strength using Charpy impact testing machine showed that impact strength of water cooled samples were higher compared to salty water cooled samples. This is due to the increased formation of martensitic structure and finer pearlite grains. The microstructure of the samples was studied using photographic visual metallurgical microscope. For low cooling rate as in the air cooled sample, the austenite was observed to transform into ferrite and pearlite. Ferrite is a body-centred cubic crystal structure of iron alloys. For higher cooling rates of water and salt water cooled samples, low temperature transformation products like bainite (an acicular microstructure which is not a phase) or martensite (a very hard form of steel crystalline structure) were formed. The salt water cooled samples had more martensite regions because of the increased cooling rate.*

Keywords: *Continuous cooling, impact strength, micro structural studies, low carbon steel*

I. INTRODUCTION

The strength of steel is influenced by its microstructure (the type of crystal patterns). The microstructure is controlled by the arrangement of the atoms of the various elements in the steel. Heating and cooling of the steel influences this atomic arrangement.

In most welding procedures metal is melted to bridge the parts to be joined so that on solidification of the weld metal the parts become united. The common processes of this type are grouped as fusion welding. Heat must be supplied to cause the melting of the filler metal and the way in which this is achieved is the major point of distinction between the different processes. The method of protecting the hot metal from the attack by the atmosphere and the cleaning or fluxing away of contaminating surface films and oxides provide the second important distinguishing feature.

Welding operations that are done in offshore environments such as the construction, building, repair and maintenance of ships, the surrounding water which is salty serves as a cooling medium. Studies have shown that depending on the environment, welding can alter the carefully designed microstructure of steels as a result of heat affected zone thermal cycles that exceed the transformation temperature. (Shome et –al, 2004). Depending upon the heating and cooling cycles involved, different types of microstructures are obtained in weld bead and the heat affected zone (HAZ). However, from weldability stand point, one advantage that low carbon steels have over medium and high carbon steels is that heat may not drastically affect the materials strength, therefore preheat can be avoided entirely or only very low temperature preheat is required, saving cost in production.

The micro constituents that are evident in the weld metal and heat affected zone of ultra low carbon steel weldments were reported by Fonda (et – al, 2000), the precipitates could either be coarsen or dissolve in the steel matrix during heating cycle, which can lead to excessive austenite grain growth in the heat affected zone due to the absence of the pinning effect of precipitates on austenite grain boundaries. The coarse grain size decreases the nucleation sites for high temperature transformation products such as ferrite and pearlite, tending to suppress their formation. If cooling rate is sufficiently high, martensite could form in the heat affected zone. When parameters such as pre-heating temperature, cooling time after welding, post weld heat treatment were varied, the results showed that it is possible to get microstructures that do not contain any untempered martensite in the heat affected zone of hardenable steels (Hernandez, 2010).

During welding, molten metal consists of a mixture of the base metal, and substances from the coating of the electrode; this mixture forms the weld when it solidifies. The electrode coating deoxidizes the weld area and provides a shielding gas to protect it from oxygen, hydrogen and nitrogen in the environment.

The Shielded metal arc welding (SMAW) process is commonly used in general construction, shipbuilding, pipelines and maintenance work. The process is suited best for work piece thicknesses of 3 to 19 mm, although this range can be extended easily by skilled operators using multiple pass techniques.

Akselsen et al. (2009) conducted a research to assess the weldability of duplex stainless steel under hyperbaric (high pressure) conditions. This was achieved by horizontal welding with Inconel 625 (Nickel-Chromium-Molybdenum alloy) wire in V-grooves on plates in 2205 duplex steel in chamber pressures of 12 and 35 bar that is, welds 1 and 2 respectively. The results from all-weld-metal tensile testing showed average yield strengths of 491 and 468 MPa (mega pascal) for Welds 1 and 2, respectively. Weld metal yield strength was lower than that of the base metal which had yield strength of 518 MPa. The tensile strength is similar to that of the base metal. The tensile strength of the base metal was 744MPa. Welds 1 and 2 had tensile strengths of 739 and 735MPa respectively. For weld 1, the weld metal toughness exceeded 150 J, while weld 2 had values slightly below 150 J. Liu et al. (2011) observed that underwater friction stir welding (underwater FSW) has been demonstrated to be available for the strength improvement of normal FSW joints. A 2219 aluminium alloy was underwater friction stir welded at a fixed rotation speed of 800 rpm and various welding speeds ranging from 50 to 200 mm/min in order to clarify the effect of welding speed on the performance of underwater friction stir welded joint. The results revealed that the precipitate deterioration in the thermal mechanically affected zone and the heat affected zone is weakened with the increase of welding speed, leading to a narrowing of softening region and an increase in lowest hardness value. Tensile strength firstly increased with the welding speed but dramatically decreased at the welding speed of 200 mm/min owing to the occurrence of groove defect. Fukuoka et al (1994) welded steel plates of sizes 2mm, 8mm, 14mm, 16mm and 19mm using gas shielded arc welding for both air and underwater welding. Cooling rate was observed to increase with increase in plate thickness with air weld recording a more consistent increase. From the results, it was observed that the hardness for underwater welding is almost twice that of the welding in air around weld metal and heat affected zone (HAZ), and remarkable differences were not observed between both welding processes in the base metal away from the weld zone. According to Calik (2009), currently, there is a strong interest in studying the effect of cooling rate on the mechanical properties and microstructure of industrial processed steels. Calik (2009) has studied the effect of cooling rate on hardness and microstructure of AISI 1020, AISI 1040, and AISI 1060 steels and shown that the microstructure of these steels can be changed and significantly improved by varying the cooling rates. Adedayo and Oyatokun (2013) studied the effect of saline water cooling on service quality of a welded AISI 1013 Carbon steel plate by varying the coolant flow rates.

Therefore, in this study the effect of simultaneous cooling (using different cooling media such as air, water and salty water (3.5percent salty in water)) and welding at varying distances from the weld fusion line on the mechanical properties and the microstructures of low carbon steel plates was investigated.

II. EXPERIMENTAL PROCEDURE

The elemental composition of the low carbon steel is presented in Table 1 as determined using X-Ray Fluorescence (XRF) at the Universal Steels, Ikeja, Lagos. The cooling media used were: air, water and salty water (3.5 percent of sodium chloride in water). Using elemental values presented in Table 1, the Carbon equivalent of the low carbon steel was calculated thus;

Carbon Equivalent (CE) = $C + \frac{Mn}{6} + \frac{Cr+Mo+V}{5} + \frac{Ni+Cu}{15}$

When the values in Table 1 are substituted into the carbon equivalent formula, 0.2046 is obtained as the carbon equivalent for the material used for the research.

Table 1: Elemental composition of the material

Element	C	Si	Mn	S	P	Cr	Ni	Cu	Nb	Al	B	W	Mo	V	Ti	Fe
Average content	**0.146**	**0.297**	**0.285**	**0.027**	**0.021**	**0.040**	**0.018**	**0.028**	**0.0001**	**0.0001**	**0.0001**	**0.0001**	**0.0001**	**0.0001**	**0.007**	**99.131**

Specimen Preparation

A total number of 108 samples were prepared from a 5mm thick plate. 54 samples were used for impact test. Metallographic examination was carried out on another set of 54 samples. The effect of continuous cooling on their mechanical property was observed at eight(8) different positions. For each cooling position T1 to T8 (with an interval of 5mm between 10mm to 45mm from the fusion zone), three samples were produced in order to obtain average values. Six (6) of the samples were used as control or standard test samples. Before the

samples were butt joint welded, they were chamfered at angles 30^o creating a vee-groove and leaving a root face and a root gap as shown in Fig.1.
All the dimensions are in millimetres (mm).

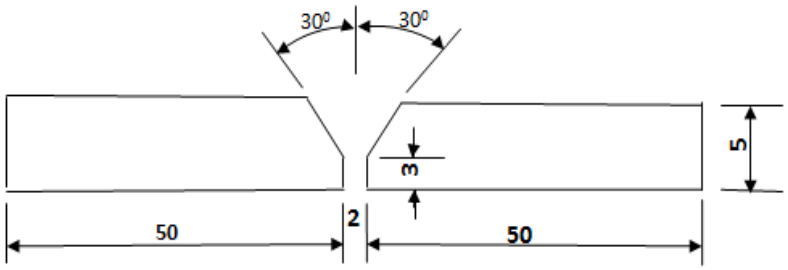

Figure 1: Sample preparation for butt (v- groove) welding

All the samples (both welded and unwelded) were cleaned from dirt and oil and a grinding machine was used to grind their surfaces before and after welding. Grinding of the surfaces was necessary to provide uniform thickness of the weld joint and other parts of the sample.

2.1 Mechanical Test

2.1.1 Impact Test

The Charpy (Balanced Impact Strength Tester) impact testing machine was utilized for impact tests of fifty-four samples. Charpy V-notches were prepared according to ASTM A370.

2.1.2 Welding Process

After sample cleaning and preparation, the samples were welded using shielded manual arc welding (SMAW) process. Core wire electrodes of standard wire gauge 12 were used. The cooling process was aided by coolant flow guide as shown in Figure 2. During the welding process, the samples were cooled simultaneously at different distances each from the fusion zone as shown in figure 3.4. The samples were cooled at distances (x) 10mm, 15mm, 20mm, and 25mm to 45mm length from the fusion zone. The accuracy of this cooling process is aided by using a coolant flow guide. Water, salt water (3.5percent sodium chloride) and air were used as cooling mediums. 72 samples were cooled with water and salt water, and nine samples in air. Temperatures at 10mm from the fusion zone were recorded for all the welded samples. After striking the electrode, it was held at an angle of 75-85 degrees to the plate and then moved steadily along the plate towards the operator and maintaining a constant height above the plate.
Welding parameters for the welding are shown it table 2.

Table 2: Welding parameters

Voltage	Current	Average Speed	Heat transfer efficiency factor f1 (for SMAW)	Heat Input	Mass Flow Rate of Coolant
18V	250A	3.1MM/S	0.65	1 453.06 J/mm	718.2 g/s

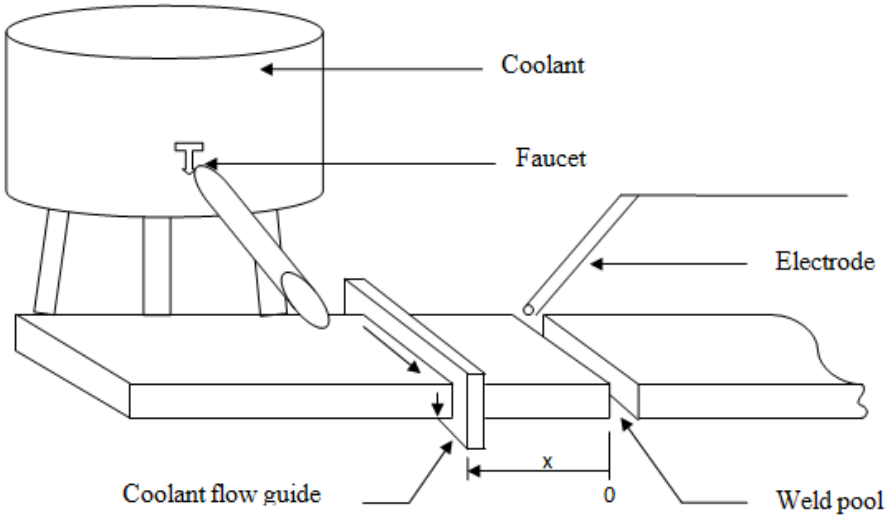

Figure 2: Experimental set-up

2.1.3 Metallurgical Examination

The sample surfaces were grinded using silicon carbide papers of various grits sizes. They are 120, 240, 320, 400 and 600. The finest grit size is 600 while the coarsest is 120. Coolant was applied simultaneously in order to avoid heating up the sample which can change its mechanical property by annealing the material. Secondly, the coolant provides a rinsing action to flush away the particles being removed from the surface.

Furthermore, the samples surfaces were polished giving rise to shiny surfaces. This was performed by applying a fine abrasive material such as synthetic alumina to a smooth, lint-free cloth polishing wheel mounted on a motor, and then robbing it on the work surface in a rotary action. During this process, the sample was rotated in a direction opposite the clockwise rotation of the wheel. Coolant was also used to keep the samples at low temperatures.

2.1.4 Etching and Microscopy

All the samples were etched using Nital. They were then examined under Photographic visual Metallurgical Microscope. The microscope was used to make visible the structural and metallographic characteristics of the samples under the different conditions of welding and cooling using a magnification of ×100.

III. RESULTS AND DISCUSSION

3.1 Cooling Curves

A typical arc weld thermal cycle consists of very rapid heating to a peak temperature, followed by relatively fast cooling to ambient temperature (Poorhaydari et al., 2005). This phenomenon is seen in the cooling curves shown below. The time it took to cool in air from 800°C to 500°C for weld was 12 seconds while for water cooled weld, it took 8 seconds. Salty water cooled welds took only 4 seconds to cool from 800^0C to 500^0C. Hence, it was observed that the cooling rate for salty water was higher than that of water then followed by air. This agrees with what Ibarra, et al, (1995) observed. The effect of these varying rates of cooling can be seen in the microstructures of the welded samples. The cooling curves were labeled from T1 to T8 representing temperatures recorded at intervals of 5mm from 45mm to 10mm towards the weld joint, respectively. The temperature at the weld zone and heat affected zone was observed to drop faster as cooling position was brought closer to the weld zone.

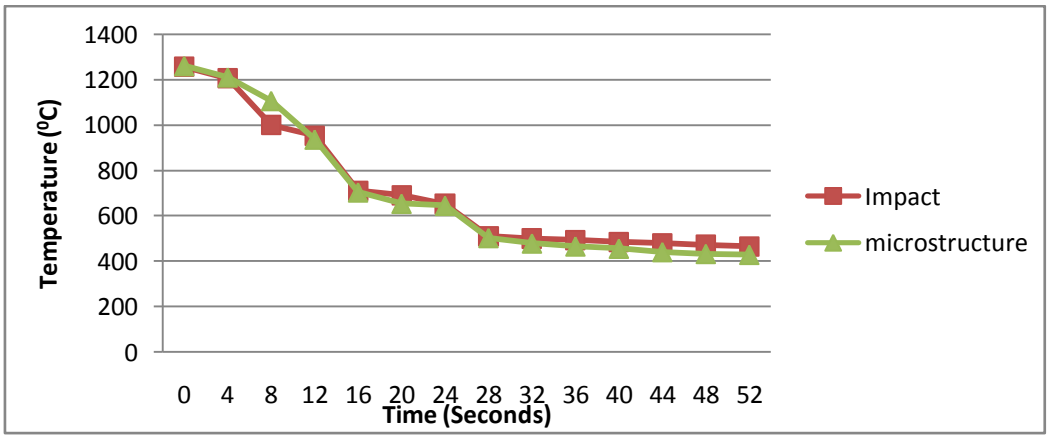

Figure 5: Air cooling curves for impact and microstructure test samples

Figure 5, presents the cooling curves of air cooled samples subjected to impact and and microstructure test. A rapid fall in temperature to about 1200^0C was observed followed by a gradual temperature fall to about 400^0C after 60 seconds.)

3.1.1 Cooling Curves for Water Cooled Samples

Water cooled: impact and microstructure test specimen cooling curves are shown in this section. It was observed in Figures 6 and 7 that temperature drops faster from curve T1 to T8. It took an average time of 8 seconds to cool the weld from 800^0C to 500^0C. It was again observed that the closer the cooling position is to the weld zone, the faster temperature drop increased because of the thermal gradient.

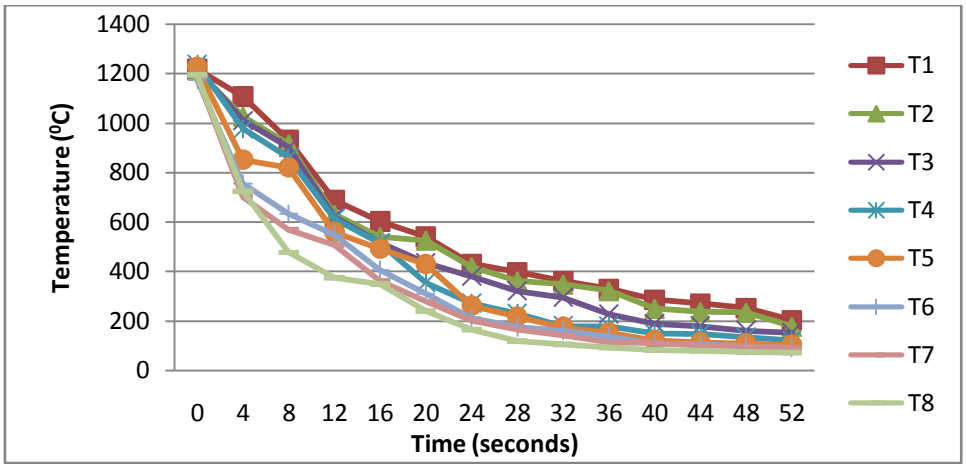

Figure 6: Impact test Curves for Water Cooled Samples

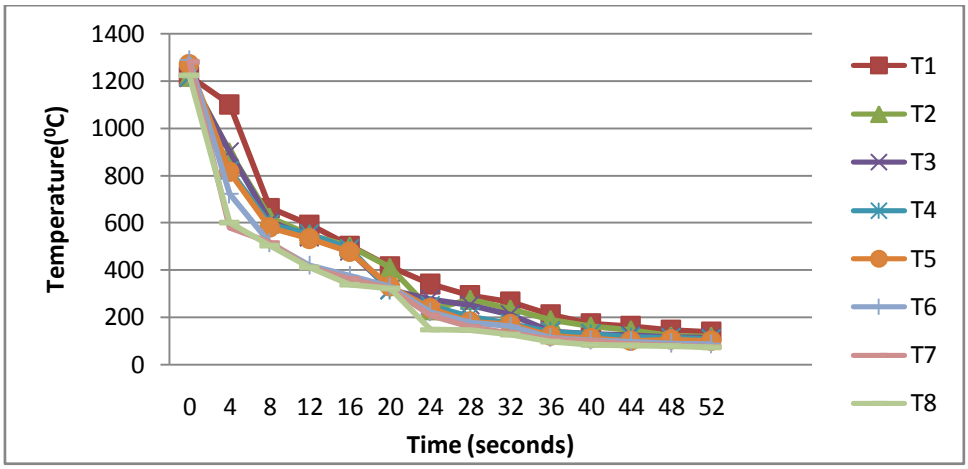

Figure 7: Microstructure Test Curves for Water Cooled Samples

The figures 6 and 7 also show that compared to air cooling curve, the temperature drop after 60 seconds was lower for the water cooled samples.

3.1.2 Cooling Curves for Salty Water Cooled Samples

In this section, salty-water cooled impact and microstructure test cooling curves are shown. It was observed from figure 8 that temperature dropped from 800^0C to 500^0C in 4 seconds. It was also observed that the closer the cooling position was to the weld zone, the faster the temperature dropped.

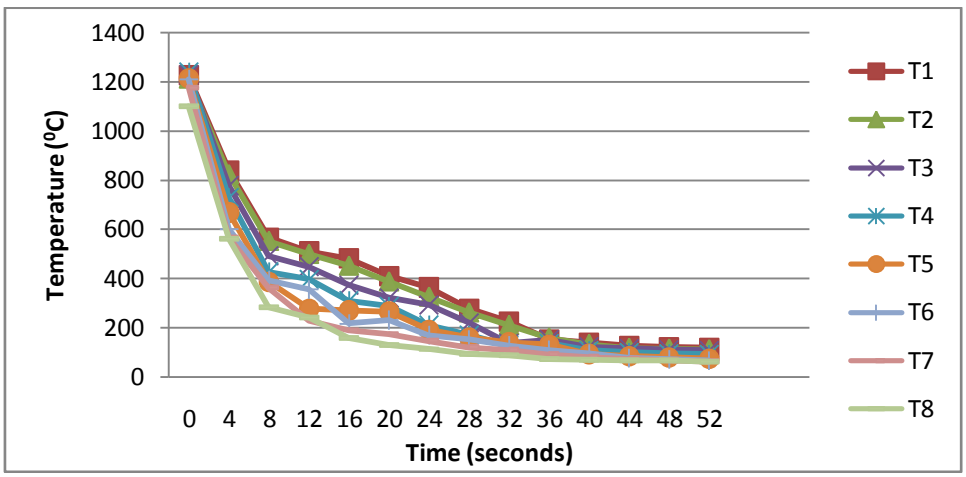

Figure 8: Impact test Curves for Salty Water Cooled Samples

From figure 8, it was observed that in about 60 seconds, the temperature dropped to about 100^0C and less. These cooling curves for salty-water cooling shows a more rapid cooling rate than air and water cooling. This rapid cooling resulted in a decrease in impact strength of the samples that were cooled with salty water. Calik (2009) has shown that the microhardness of steels increases with the cooling rate and also carbon content. Additionally, the microhardness increases with increasing pearlite percentage. Their microstructure also showed a decrease in the amount of ferrites.The cooling curves show that cooling distance from weld zone has minimal effect on peak temperature but it has influence on cooling rate.

3.2 Mechanical properties:

3.2.1 Impact Energy

Table 2 shows the impact test results for the air cooled sample and the control sample.
Impact energy values of water and salt water cooled samples are presented in Tables 2 and 3.

Table 2: Air Cooled Sample and Control sample

	Impact energy (Joules)
Air	**16.95**
Control Sample	**18.98**

Table 3: Impact Energy Values for Water Cooled samples

Distance from weld (mm)	Impact energy (Joules)
10	**12.88**
15	**13.56**
20	**14.92**
25	**18.31**
30	**19.26**
35	**21.70**
40	**21.70**
45	**25.09**

Table 4: Impact Energy Values for Salt Water Cooled Samples

Distance from weld (mm)	Impact energy (Joules)
10	**11.66**
15	**12.20**
20	**12.88**
25	**14.51**
30	**16.95**
35	**17.09**
40	**17.63**
45	**18.31**

Impact test results of water cooled samples and salty water cooled samples are presented in Figure 10.

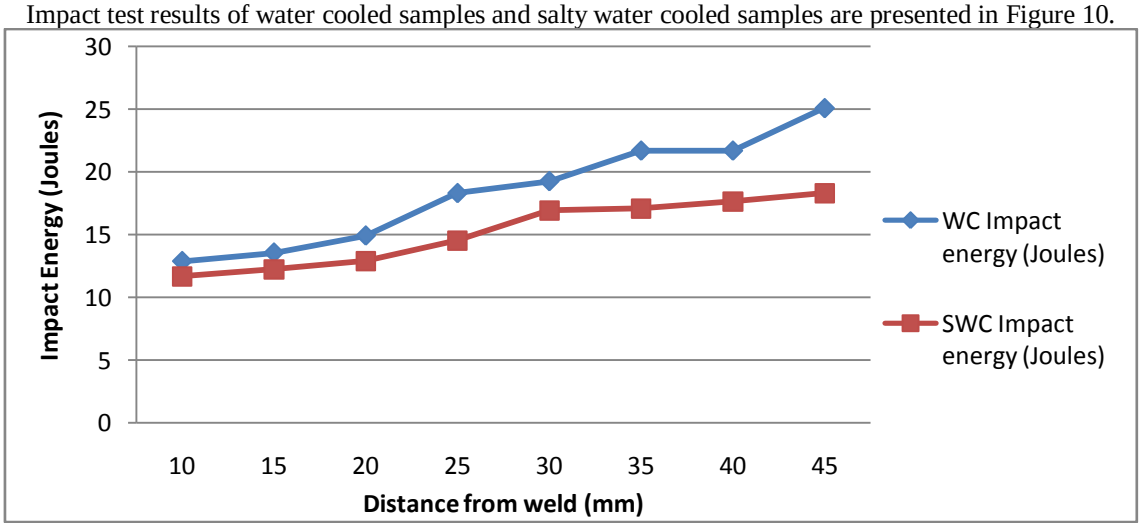

Figure 10: Variation of Impact Energy and Distance of Weld of Samples.

Figure 10 shows that increased rate of cooling has a negative effect on toughness of the low carbon steel. Toughness values of the water cooled samples are higher than the values of the samples that were cooled in salty water. This is due to the increased formation of martensitic structure and finer pearlite grains.

3.2.2 Microstructures

The microstructures of control, air, water and salty water cooled samples are presented in this section with a magnification of ×100.

Plate 1: Control sample

The control sample in plate 1 shows ferrite and pearlite layers because of the low carbon content in the material and the grain structure is coarse. The ferrites are the white areas while pearlites are the dark areas.

a, Air Weld

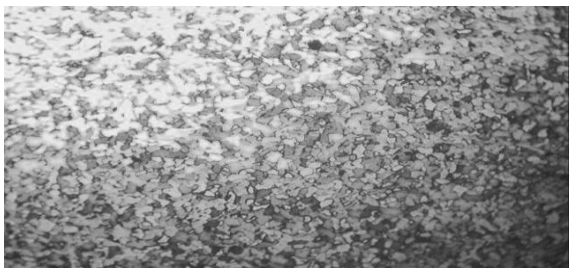

b, Air HAZ

Plate 2: Weld zone and Heat Affected Zone (cooled under room temperature)

In plate 2, the weld zone has fine grains while the heat affected zone has coarse grains. This is because of the faster cooling rate at the weld zone. There is no sufficient time for grain growth and nucleation in the weld zone.

3.2.2.1 Heat Affected Zone (Water)

Ibarra, et al, (1995), observed in his work that due to the rapid cooling that occurs in wet weld, the heat affected zone of most welded mild steel are coarse-grained and martensitic. This was also observed in the heat affected zone micrographs shown in plate 3 and plate 4. The salty water cooled samples have more martensitic structures than water and air cooled samples.

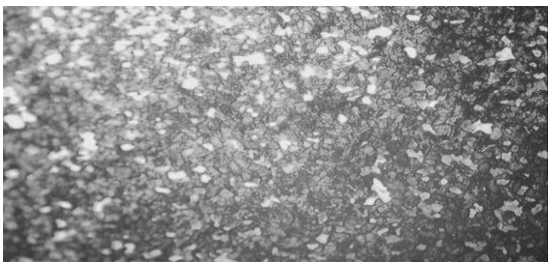

10mm

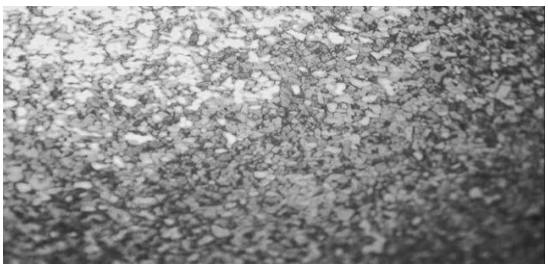

15mm

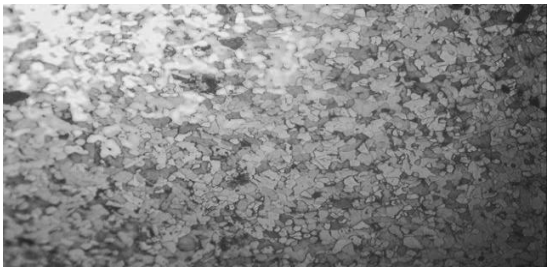

40mm

45mm

Plate 3: Heat Affected Zone (Water Cooled)

From the micrographs presented in plate 3, at 45mm from the weld, ferrite structure is seen to be more and generally dispersed in the microstructure. The ferrite structures are the light-coloured regions of the structure.

The amount of pearlite was observed to increase as the cooling distance from the weld reduces (that is, as the material is cooled at a distance nearer to the weld zone).

3.2.2.2 Heat Affected Zone (salty water)

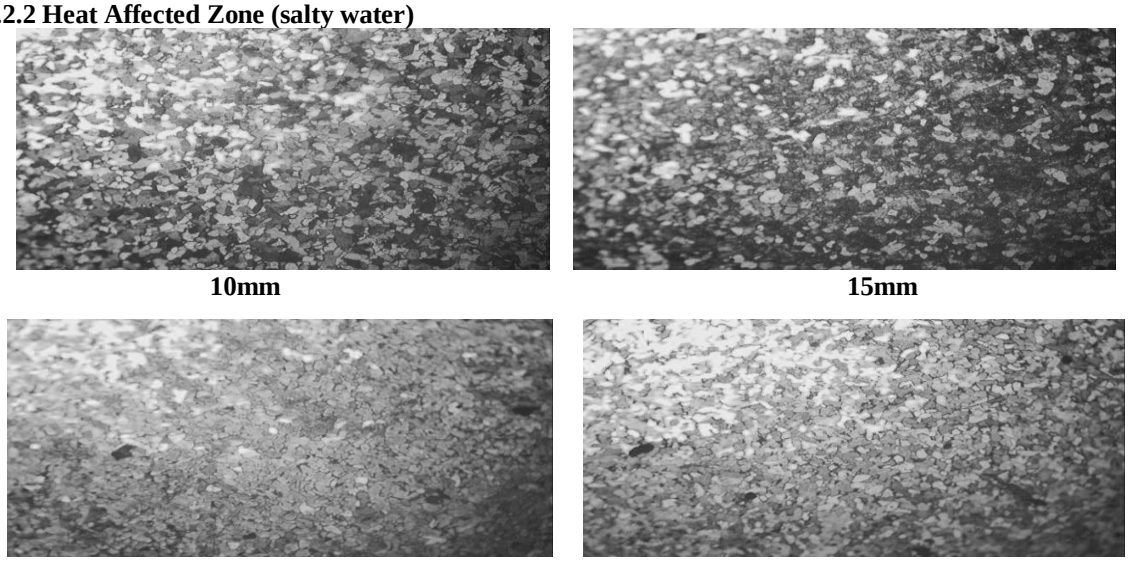

10mm **15mm**

40mm **45mm**

Plate 4: Heat Affected Zone (Salty Water Cooled)

The micrographs presented in this section show the samples cooled in 3.5percent salty in water. The cooling rate is faster than water cooling. The grains are also coarse but it was observed that there is an increase, though minimal, in the amount of pearlite layers. At 10mm and 15mm from the weld zone, martensitic structures were noticed.

3.2.2.3 Weld (water)

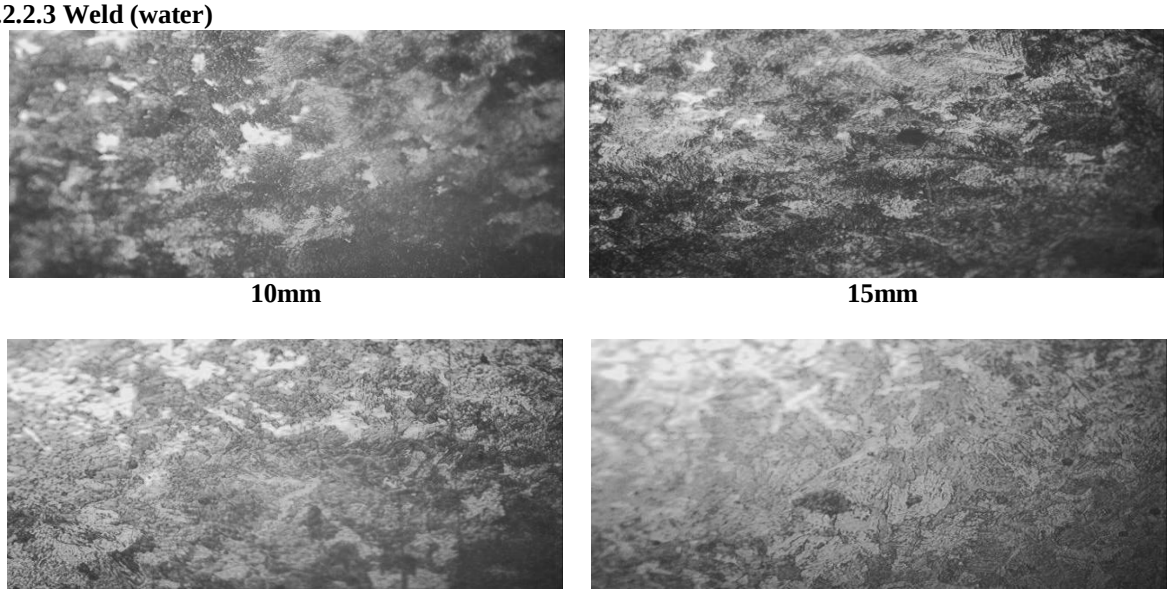

10mm **15mm**

40mm **45mm**

Plate 5: Weld Zone Microstructures (Water Cooled)

Weld zone microstructures when water cooled are presented in plate 5. The grain structures are fine and finger-like. This is because of the rapid cooling rate at the weld zone. The micrographs farther away from the weld show more ferrite structures and some few pearlite layers.

3.2.2.4 Weld (salty water)

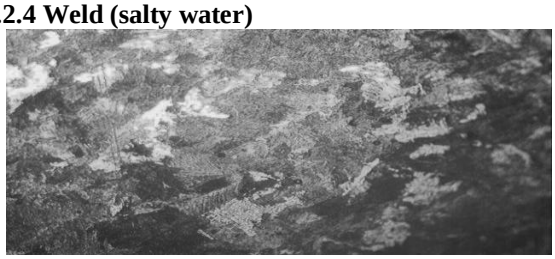

10mm

15mm

40mm

45mm

Plate 6: Weld Zone Microstructures (Salty Water Cooled)

The micrographs above (plate 6), are also fine grained. The microstructure of the 10mm and 15mm samples show some martensitic layers with some pearlite regions. It was observed that the martensite in the water cooled weld micrographs are more evenly dispersed than that of the salty water cooled weld zone micrographs. The microstructures of samples cooled far from the weld zone are also more ferritic. The increase in pearlite and martensite in the salty water cooled samples results in a decrease in their impact strength.

3.2.3 Comparison of Microstructure for the Different Cooling Media

The peak temperature of the weld zone and heat affected zone exceeds the lower critical temperature A_1 (723^0C) as shown in plate 1 to plate 6. Temperature readings were taken at 10mm from fusion zone of the weld. Ferrite, which has a body centred cubic (bcc) structure transforms into austenite (a high temperature phase with face centred cubic (fcc) crystal structure). During the cooling cycle, the austenite transforms back into ferrite or other metastable phases as seen in plate 2.

For low cooling rate as in the air cooled sample, the austenite was observed to transform into ferrite. For higher cooling rates of water and salty water cooled samples, low temperature transformation products like bainite or martensite were formed. The salty water cooled samples had more martensite regions because of the increased cooling rate (see plate 4 and 6). Temperature dropped from 800^0C to 500^0C in 4seconds in salty water cooling compared to 8 seconds for water cooling and 12 seconds in air cooling for the same temperature ranges of 800^0C to 500^0C. As the cooling rate in the weld zone and heat affected zone varied with cooling distance from the fusion zone of the weld, the phases formed from the transformation was observed to also vary with cooling distance. From the impact test results, the coarse grained heat affected zone (CGHAZ) had poor toughness properties compared to the rest of the heat affected zone (HAZ) and unaffected areas of the steel because of the large grain size and high cooling rate in the region.

IV. CONCLUSION

The following conclusions were drawn:

1. The samples cooled with salty water had lower impact strength values possibly due to the formation of martensitic structure after quenching, while, air cooled samples were mostly ferrite. Samples cooled with water had higher impact strength values. Improved toughness values were observed for water cooled samples between 30mm to 45mm cooling distance from the weld zone.
2. Cooling distance between 30mm to 35mm provided optimum impact strength.
3. It was observed that the variations in the microstructures were minimal. This was possibly due to the rapid heat input, very short soaking time during welding and the low carbon content of the material.
4. It was noticed that impact strength of the low carbon steel reduced with increasing cooling rate.
5. Furthermore, the closer the cooling position, the more the cooling effect and the more the mechanical and metallurgical properties were influenced.
6. Wet underwater welding should be avoided in environments containing high salty concentration because of their rapid cooling effect compared to ordinary water.

REFERENCES

[1]. Adedayo, S.M. and Oyatokun, V.O. (2013) Effect of saline water cooling on service quality of a welded AISI 1013 Carbon steel plate. Annals of faculty of engineering Hunedoara-International Journal of Engineering, Tome XI, Fascicule 2

[2]. Akselsen O. M., Fostervoll H. And Ahlen C. H. (2009), Hyperbaric GMA Welding of Duplex Stainless Steel at 12 and 35 bar, Supplement to the Welding Journal, American Welding Society and the Welding Research Council. PP 1-8.

[3]. Calik, A.(2009) Effect of cooling rates on the hardness and microstructure of AISI 1020, AISI 1040, and AISI 1060 steels, International Journal of Physical Sciences Vol.4(9),pp 514-518. Available online at hhtp://www.academicjournals.org/IJPS

[4]. Fonda R. W and Spanos. G (2000) Micrstructural evolution in ultra low carbon steel weldments-Part 1: Controlled thermal cycling and continuous cooling transformation diagram of weld metal. Metallurgical and Materials Transaction. A31A- Pp 2145- 2153

[5]. Fukuoka T. and Fukui S. (1994), Analysis for Cooling Process of Underwater Welding -Comparison with Welding in Air, Bulletin of the M.E.S.J., Vo1. 22, No.2. PP 88-92.

[6]. Ibarra S., Liu S. and Olson D.L., (1995), "Underwater Wet Welding of Steels", Welding Research Council Bulletin, no. 401, PP 1-39.

[7]. Keats D.J. (2009). Underwater Wet Welding Made Simple: Benefits of Hammerhead Wet-Spot Welding Process. International Journal of the Society for Underwater Technology. Vol 28, No 3. doi:10.3723/ut.28.115. PP 115-127.

[8]. Kou S. (2003). Welding Metallurgy. 2nd Edition, John Willey and Sons Inc., U.S.A. PP. 13-30

[9]. Liu H.J., Zhang H.J., and Yu L. (2011). Homogeneity of Mechanical Properties of Underwater Friction Stir Welded 2219-T6 Aluminum Alloy**.** Journal of Materials Engineering and Performance. Volume 20, Issue 8, pp 1419-1422.

[10]. Odusote,J.K., Ajiboye,T.K. and Rabiu,A.B. (2012)Evaluation of Mechanical Properties of Medium Carbon SteelQuenched in Water and Oil AU J.T. 15(4): 218-224 (Apr. 2012)

[11]. Oyetunji A. (2012) Effects of Microstructures and Process Variables on the Mechanical Properties of Rolled Ribbed Medium Carbon Steel Journal of Emerging Trends in Engineering and Applied Sciences (JETEAS) 3 (3):507-512 jeteas.scholarlinkresearch.org Assessed on 28/06/2013

[12]. Poorhaydari K, Patchett B. M., and Ivey D. G. (2005). Estimation of Cooling Rate in the Welding of Plates with Intermediate Thickness, supplement to the welding journal. PP. 4-10

[13]. Shome , M., Gupta, O. P andMohanty, O. N (2004) A modified anatytical approach for modelling grain growth in the coarse grain HAZ of HSLA teels. Scripta Materialla 50: Pp 1007- 1010